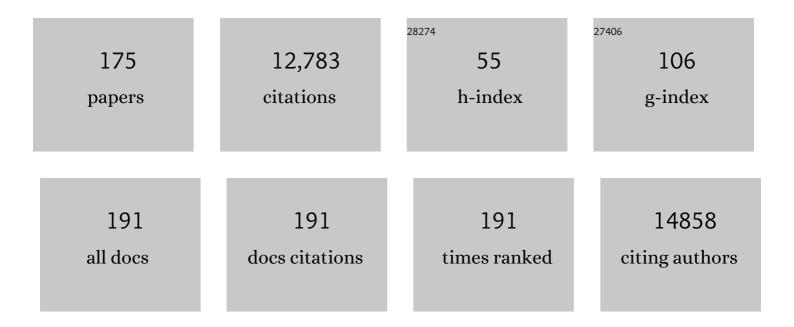
List of Publications by Year in descending order

Source: https://exaly.com/author-pdf/5014266/publications.pdf Version: 2024-02-01



Номстні Шлис

#	Article	IF	CITATIONS
1	Design and Mechanisms of Asymmetric Supercapacitors. Chemical Reviews, 2018, 118, 9233-9280.	47.7	2,379
2	Graphene-based materials for flexible supercapacitors. Chemical Society Reviews, 2015, 44, 3639-3665.	38.1	1,015
3	3D Freezeâ€Casting of Cellular Graphene Films for Ultrahighâ€Powerâ€Density Supercapacitors. Advanced Materials, 2016, 28, 6719-6726.	21.0	390
4	Origami-inspired active graphene-based paper for programmable instant self-folding walking devices. Science Advances, 2015, 1, e1500533.	10.3	312
5	Highly Conductive, Flexible, and Compressible Allâ€Graphene Passive Electronic Skin for Sensing Human Touch. Advanced Materials, 2014, 26, 5018-5024.	21.0	273
6	Flexible quasi-solid-state planar micro-supercapacitor based on cellular graphene films. Materials Horizons, 2017, 4, 1145-1150.	12.2	222
7	Sheath-run artificial muscles. Science, 2019, 365, 150-155.	12.6	218
8	Earth-Abundant Oxygen Electrocatalysts for Alkaline Anion-Exchange-Membrane Water Electrolysis: Effects of Catalyst Conductivity and Comparison with Performance in Three-Electrode Cells. ACS Catalysis, 2019, 9, 7-15.	11.2	189
9	Ultrathin, Washable, and Largeâ€Area Graphene Papers for Personal Thermal Management. Small, 2017, 13, 1702645.	10.0	177
10	Advanced Functional Fiber and Smart Textile. Advanced Fiber Materials, 2019, 1, 3-31.	16.1	169
11	Molecular-channel driven actuator with considerations for multiple configurations and color switching. Nature Communications, 2018, 9, 590.	12.8	159
12	High-performance flexible asymmetric supercapacitors based on 3D porous graphene/MnO ₂ nanorod and graphene/Ag hybrid thin-film electrodes. Journal of Materials Chemistry C, 2013, 1, 1245-1251.	5.5	156
13	An Elastic Transparent Conductor Based on Hierarchically Wrinkled Reduced Graphene Oxide for Artificial Muscles and Sensors. Advanced Materials, 2016, 28, 9491-9497.	21.0	147
14	Flexible and high-performance electrochromic devices enabled by self-assembled 2D TiO2/MXene heterostructures. Nature Communications, 2021, 12, 1587.	12.8	143
15	Morphology-tailored synthesis of vertically aligned 1D WO ₃ nano-structure films for highly enhanced electrochromic performance. Journal of Materials Chemistry A, 2013, 1, 684-691.	10.3	140
16	lon-Transport Design for High-Performance Na ⁺ -Based Electrochromics. ACS Nano, 2018, 12, 3759-3768.	14.6	136
17	MXene-conducting polymer electrochromic microsupercapacitors. Energy Storage Materials, 2019, 20, 455-461.	18.0	136
18	Fluoroalkylsilane-Modified Textile-Based Personal Energy Management Device for Multifunctional Wearable Applications. ACS Applied Materials & Interfaces, 2016, 8, 4676-4683.	8.0	130

#	Article	IF	CITATIONS
19	Enhanced Power Output of a Triboelectric Nanogenerator Composed of Electrospun Nanofiber Mats Doped with Graphene Oxide. Scientific Reports, 2015, 5, 13942.	3.3	123
20	Continuous and scalable manufacture of amphibious energy yarns and textiles. Nature Communications, 2019, 10, 868.	12.8	121
21	All-fiber tribo-ferroelectric synergistic electronics with high thermal-moisture stability and comfortability. Nature Communications, 2019, 10, 5541.	12.8	121
22	A highly integrated sensing paper for wearable electrochemical sweat analysis. Biosensors and Bioelectronics, 2021, 174, 112828.	10.1	113
23	MXene-Coated Air-Permeable Pressure-Sensing Fabric for Smart Wear. ACS Applied Materials & Interfaces, 2020, 12, 46446-46454.	8.0	111
24	Aluminumâ€ionâ€intercalation Supercapacitors with Ultrahigh Areal Capacitance and Highly Enhanced Cycling Stability: Power Supply for Flexible Electrochromic Devices. Small, 2017, 13, 1700380.	10.0	107
25	Microfluidic Crystal Engineering of ï€-Conjugated Polymers. ACS Nano, 2015, 9, 8220-8230.	14.6	102
26	High-performance all-solid-state yarn supercapacitors based on porous graphene ribbons. Nano Energy, 2015, 12, 26-32.	16.0	101
27	Cladding nanostructured AgNWs-MoS2 electrode material for high-rate and long-life transparent in-plane micro-supercapacitor. Energy Storage Materials, 2019, 16, 212-219.	18.0	99
28	Hierarchical NiO microflake films with high coloration efficiency, cyclic stability and low power consumption for applications in a complementary electrochromic device. Nanoscale, 2013, 5, 4808.	5.6	97
29	Red, Green, Blue (RGB) Electrochromic Fibers for the New Smart Color Change Fabrics. ACS Applied Materials & Interfaces, 2014, 6, 13043-13050.	8.0	97
30	Highâ€Performance Flexible Thermoelectric Devices Based on Allâ€Inorganic Hybrid Films for Harvesting Lowâ€Grade Heat. Advanced Functional Materials, 2019, 29, 1900304.	14.9	97
31	Fluorinated metal-organic framework as bifunctional filler toward highly improving output performance of triboelectric nanogenerators. Nano Energy, 2020, 70, 104517.	16.0	97
32	A Moisture-Wicking Passive Radiative Cooling Hierarchical Metafabric. ACS Nano, 2022, 16, 2188-2197.	14.6	96
33	A multi-responsive water-driven actuator with instant and powerful performance for versatile applications. Scientific Reports, 2015, 5, 9503.	3.3	91
34	Synergistic Solvation and Interface Regulations of Ecoâ€Friendly Silk Peptide Additive Enabling Stable Aqueous Zincâ€Ion Batteries. Advanced Functional Materials, 2022, 32, .	14.9	91
35	Regulation of carbon content in MOF-derived hierarchical-porous NiO@C films for high-performance electrochromism. Materials Horizons, 2019, 6, 571-579.	12.2	90
36	S, N Co-Doped Graphene Quantum Dot/TiO2 Composites for Efficient Photocatalytic Hydrogen Generation. Nanoscale Research Letters, 2017, 12, 400.	5.7	87

#	Article	IF	CITATIONS
37	Stable Hydrogel Electrolytes for Flexible and Submarine-Use Zn-Ion Batteries. ACS Applied Materials & Interfaces, 2020, 12, 46005-46014.	8.0	87
38	Infrared-Radiation-Enhanced Nanofiber Membrane for Sky Radiative Cooling of the Human Body. ACS Applied Materials & Interfaces, 2019, 11, 44673-44681.	8.0	82
39	Lattice-contraction triggered synchronous electrochromic actuator. Nature Communications, 2018, 9, 4798.	12.8	80
40	Facilitating Interfacial Stability Via Bilayer Heterostructure Solid Electrolyte Toward Highâ€energy, Safe and Adaptable Lithium Batteries. Advanced Energy Materials, 2020, 10, 2000709.	19.5	79
41	Bio-applicable and electroactive near-infrared laser-triggered self-healing hydrogels based on graphene networks. Journal of Materials Chemistry, 2012, 22, 14991.	6.7	76
42	A wearable, fibroid, self-powered active kinematic sensor based on stretchable sheath-core structural triboelectric fibers. Nano Energy, 2017, 39, 673-683.	16.0	71
43	Self-seeded growth of nest-like hydrated tungsten trioxide film directly on FTO substrate for highly enhanced electrochromic performance. Journal of Materials Chemistry A, 2014, 2, 11305-11310.	10.3	70
44	Abrasion Resistant/Waterproof Stretchable Triboelectric Yarns Based on Fermat Spirals. Advanced Materials, 2021, 33, e2100782.	21.0	68
45	Facile growth of vertically aligned BiOCl nanosheet arrays on conductive glass substrate with high photocatalytic properties. Journal of Materials Chemistry, 2012, 22, 16851.	6.7	67
46	Graphene papers: smart architecture and specific functionalization for biomimetics, electrocatalytic sensing and energy storage. Materials Chemistry Frontiers, 2017, 1, 37-60.	5.9	67
47	Bipolar carbide-carbon high voltage aqueous lithium-ion capacitors. Nano Energy, 2019, 56, 151-159.	16.0	67
48	Cobalt nitride nanoparticle coated hollow carbon spheres with nitrogen vacancies as an electrocatalyst for lithium–sulfur batteries. Journal of Materials Chemistry A, 2020, 8, 14498-14505.	10.3	66
49	Self-weaving WO3 nanoflake films with greatly enhanced electrochromic performance. Journal of Materials Chemistry, 2012, 22, 16633.	6.7	65
50	A high efficiency microreactor with Pt/ZnO nanorod arrays on the inner wall for photodegradation of phenol. Journal of Hazardous Materials, 2013, 254-255, 318-324.	12.4	65
51	Modifying Perovskite Films with Polyvinylpyrrolidone for Ambient-Air-Stable Highly Bendable Solar Cells. ACS Applied Materials & Interfaces, 2018, 10, 35385-35394.	8.0	64
52	Spray coated ultrathin films from aqueous tungsten molybdenum oxide nanoparticle ink for high contrast electrochromic applications. Journal of Materials Chemistry C, 2016, 4, 33-38.	5.5	63
53	Engineering two-dimensional layered nanomaterials for wearable biomedical sensors and power devices. Materials Chemistry Frontiers, 2018, 2, 1944-1986.	5.9	59
54	Selfâ€Powered Interactive Fiber Electronics with Visual–Digital Synergies. Advanced Materials, 2021, 33, e2104681.	21.0	58

#	Article	IF	CITATIONS
55	Wearable Thermoelectric Devices Based on Au-Decorated Two-Dimensional MoS ₂ . ACS Applied Materials & Interfaces, 2018, 10, 33316-33321.	8.0	57
56	A highly ionic conductive poly(methyl methacrylate) composite electrolyte with garnet-typed Li6.75La3Zr1.75Nb0.25O12 nanowires. Chemical Engineering Journal, 2019, 375, 121922.	12.7	57
57	Hierarchical Compositeâ€Solidâ€Electrolyte with High Electrochemical Stability and Interfacial Regulation for Boosting Ultraâ€Stable Lithium Batteries. Advanced Functional Materials, 2021, 31, .	14.9	57
58	Controllable growth of high-quality metal oxide/conducting polymer hierarchical nanoarrays with outstanding electrochromic properties and solar-heat shielding ability. Journal of Materials Chemistry A, 2014, 2, 13541-13549.	10.3	56
59	Structural colored fiber fabricated by a facile colloid self-assembly method in micro-space. Chemical Communications, 2011, 47, 12801.	4.1	55
60	MoS2/C/C nanofiber with double-layer carbon coating for high cycling stability and rate capability in lithium-ion batteries. Nano Research, 2018, 11, 5866-5878.	10.4	55
61	Tunable stable operating potential window for high-voltage aqueous supercapacitors. Nano Energy, 2019, 63, 103848.	16.0	55
62	Facile fabrication of a magnetically induced structurally colored fiber and its strain-responsive properties. Journal of Materials Chemistry A, 2015, 3, 11093-11097.	10.3	54
63	Highly Integrable Thermoelectric Fiber. ACS Applied Materials & amp; Interfaces, 2020, 12, 33297-33304.	8.0	54
64	Highly Strong and Elastic Graphene Fibres Prepared from Universal Graphene Oxide Precursors. Scientific Reports, 2014, 4, 4248.	3.3	53
65	Wicking–Polarizationâ€Induced Water Cluster Size Effect on Triboelectric Evaporation Textiles. Advanced Materials, 2021, 33, e2007352.	21.0	53
66	Dual-Mechanism and Multimotion Soft Actuators Based on Commercial Plastic Film. ACS Applied Materials & Interfaces, 2018, 10, 15122-15128.	8.0	52
67	Structurally colored carbon fibers with controlled optical properties prepared by a fast and continuous electrophoretic deposition method. Nanoscale, 2013, 5, 6917.	5.6	51
68	Aqueous synthesis of high bright and tunable near-infrared AgInSe 2 –ZnSe quantum dots for bioimaging. Journal of Colloid and Interface Science, 2016, 463, 1-7.	9.4	49
69	Constructing three-dimensional quasi-vertical nanosheet architectures from self-assemble two-dimensional WO 3 ·2H 2 O for efficient electrochromic devices. Applied Surface Science, 2016, 380, 281-287.	6.1	48
70	Solutionâ€Processed Porous Tungsten Molybdenum Oxide Electrodes for Energy Storage Smart Windows. Advanced Materials Technologies, 2017, 2, 1700047.	5.8	48
71	Grain engineering by ultrasonic substrate vibration post-treatment of wet perovskite films for annealing-free, high performance, and stable perovskite solar cells. Nanoscale, 2018, 10, 8526-8535.	5.6	48
72	Continuously Processed, Long Electrochromic Fibers with Multi-Environmental Stability. ACS Applied Materials & Interfaces, 2020, 12, 28451-28460.	8.0	48

#	Article	IF	CITATIONS
73	Fabrication of large-area and high-crystallinity photoreduced graphene oxide films via reconstructed two-dimensional multilayer structures. NPG Asia Materials, 2014, 6, e119-e119.	7.9	47
74	Flexible and thermostable thermoelectric devices based on large-area and porous all-graphene films. Carbon, 2016, 107, 146-153.	10.3	47
75	Hydrophobic coating over a CH ₃ NH ₃ PbI ₃ absorbing layer towards air stable perovskite solar cells. Journal of Materials Chemistry C, 2016, 4, 6848-6854.	5.5	47
76	Prepolymerization-assisted fabrication of an ultrathin immobilized layer to realize a semi-embedded wrinkled AgNW network for a smart electrothermal chromatic display and actuator. Journal of Materials Chemistry C, 2017, 5, 9778-9785.	5.5	46
77	Self-powered multifunctional UV and IR photodetector as an artificial electronic eye. Journal of Materials Chemistry C, 2017, 5, 1436-1442.	5.5	45
78	1T-Molybdenum disulfide/reduced graphene oxide hybrid fibers as high strength fibrous electrodes for wearable energy storage. Journal of Materials Chemistry A, 2019, 7, 3143-3149.	10.3	45
79	A remote controllable fiber-type near-infrared light-responsive actuator. Chemical Communications, 2017, 53, 11118-11121.	4.1	43
80	SnO2 nanorod arrays with tailored area density as efficient electron transport layers for perovskite solar cells. Journal of Power Sources, 2018, 402, 460-467.	7.8	42
81	Reduced graphene oxide functionalized stretchable and multicolor electrothermal chromatic fibers. Journal of Materials Chemistry C, 2017, 5, 11448-11453.	5.5	41
82	Tuning the reactivity of PbI2 film via monolayer Ti3C2Tx MXene for two-step-processed CH3NH3PbI3 solar cells. Chemical Engineering Journal, 2021, 417, 127912.	12.7	40
83	Thermochromic Hydrogel-Functionalized Textiles for Synchronous Visual Monitoring of On-Demand <i>In Vitro</i> Drug Release. ACS Applied Materials & Interfaces, 2020, 12, 51225-51235.	8.0	39
84	1-Ethyl-3-methylimidazolium tetrafluoroborate-doped high ionic conductivity gel electrolytes with reduced anodic reaction potentials for electrochromic devices. Materials and Design, 2017, 118, 279-285.	7.0	38
85	Versatile mechanically strong and highly conductive chemically converted graphene aerogels. Carbon, 2017, 125, 352-359.	10.3	38
86	High-performance solar cells with induced crystallization of perovskite by an evenly distributed CdSe quantum dots seed-mediated underlayer. Journal of Power Sources, 2018, 376, 46-54.	7.8	38
87	High performance stretchable fibrous supercapacitors and flexible strain sensors based on CNTs/MXene-TPU hybrid fibers. Electrochimica Acta, 2021, 395, 139141.	5.2	38
88	In Situ Functionalization of Stable 3D Nest‣ike Networks in Confined Channels for Microfluidic Enrichment and Detection. Advanced Functional Materials, 2014, 24, 1017-1026.	14.9	37
89	Thermally Responsive Photonic Fibers Consisting of Chained Nanoparticles. ACS Applied Materials & Interfaces, 2020, 12, 50844-50851.	8.0	37
90	A novel efficient ZnO/Zn(OH)F nanofiber arrays-based versatile microfluidic system for the applications of photocatalysis and histidine-rich protein separation. Sensors and Actuators B: Chemical, 2016, 229, 281-287.	7.8	35

#	Article	IF	CITATIONS
91	Lightweight, highly bendable and foldable electrochromic films based on all-solution-processed bilayer nanowire networks. Journal of Materials Chemistry C, 2016, 4, 5849-5857.	5.5	34
92	A single-walled carbon nanotubes/poly(3,4-ethylenedioxythiophene)-poly(styrenesulfonate)/copper hexacyanoferrate hybrid film for high-volumetric performance flexible supercapacitors. Journal of Power Sources, 2018, 386, 96-105.	7.8	34
93	Construction of hydrated tungsten trioxide nanosheet films for efficient electrochromic performance. RSC Advances, 2015, 5, 196-201.	3.6	33
94	Highâ€Performance Ionic Thermoelectric Supercapacitor for Integrated Energy Conversionâ€Storage. Energy and Environmental Materials, 2022, 5, 954-961.	12.8	33
95	Transparent Metal–Organic Framework-Based Gel Electrolytes for Generalized Assembly of Quasi-Solid-State Electrochromic Devices. ACS Applied Materials & Interfaces, 2020, 12, 42955-42961.	8.0	32
96	Hydrophobic SiO ₂ Electret Enhances the Performance of Poly(vinylidene fluoride) Nanofiber-Based Triboelectric Nanogenerator. Journal of Physical Chemistry C, 2016, 120, 26600-26608.	3.1	31
97	Largeâ€Grained Perovskite Films Enabled by Oneâ€Step Meniscusâ€Assisted Solution Printing of Crossâ€Aligned Conductive Nanowires for Biodegradable Flexible Solar Cells. Advanced Energy Materials, 2020, 10, 2001185.	19.5	31
98	Flexible 3D Porous MoS ₂ /CNTs Architectures with <i>ZT</i> of 0.17 at Room Temperature for Wearable Thermoelectric Applications. Advanced Functional Materials, 2020, 30, 2002508.	14.9	31
99	Metal–Organic Frameworkâ€Derived Nickel/Cobaltâ€Based Nanohybrids for Sensing Nonâ€Enzymatic Glucose. ChemElectroChem, 2020, 7, 4446-4452.	3.4	30
100	Liquid-liquid interface assisted synthesis of SnO2 nanorods with tunable length for enhanced performance in dye-sensitized solar cells. Electrochimica Acta, 2017, 227, 49-60.	5.2	28
101	Enhanced immunofluorescence detection of a protein marker using a PAA modified ZnO nanorod array-based microfluidic device. Nanoscale, 2018, 10, 17663-17670.	5.6	28
102	Highly sensitive microfluidic detection of carcinoembryonic antigen via a synergetic fluorescence enhancement strategy based on the micro/nanostructure optimization of ZnO nanorod arrays and in situ ZIF-8 coating. Chemical Engineering Journal, 2020, 383, 123230.	12.7	28
103	Fabrication of magnetic field induced structural colored films with tunable colors and its application on security materials. Journal of Colloid and Interface Science, 2017, 485, 18-24.	9.4	27
104	Skeleton-Structure WS2@CNT Thin-Film Hybrid Electrodes for High-Performance Quasi-Solid-State Flexible Supercapacitors. Frontiers in Chemistry, 2020, 8, 442.	3.6	27
105	Layer-by-layer assembled triphenylene-based MOFs films for electrochromic electrode. Inorganic Chemistry Communication, 2021, 123, 108354.	3.9	27
106	One-pot Hydrothermal Synthesis of N-Doped Carbon Quantum Dots Using the Waste of Shrimp for Hydrogen Evolution from Formic Acid. Chemistry Letters, 2015, 44, 241-243.	1.3	26
107	Conjugated Polymer Alignment: Synergisms Derived from Microfluidic Shear Design and UV Irradiation. ACS Applied Materials & Interfaces, 2016, 8, 24761-24772.	8.0	26
108	Facile fabrication of magnetically responsive PDMS fiber for camouflage. Journal of Colloid and Interface Science, 2016, 483, 11-16.	9.4	26

#	Article	IF	CITATIONS
109	Calligraphy-inspired brush written foldable supercapacitors. Nano Energy, 2017, 38, 428-437.	16.0	26
110	Enhanced Piezoelectric Performance of Electrospun Polyvinylidene Fluoride Doped with Inorganic Salts. Macromolecular Materials and Engineering, 2017, 302, 1700214.	3.6	26
111	A kirigami-inspired island-chain design for wearable moistureproof perovskite solar cells with high stretchability and performance stability. Nanoscale, 2020, 12, 3646-3656.	5.6	26
112	Emerging Two-dimensional Materials Constructed Nanofluidic Fiber: Properties, Preparation and Applications. Advanced Fiber Materials, 2022, 4, 129-144.	16.1	26
113	Graphene-carbon nanotube papers for energy conversion and storage under sunlight and heat. Carbon, 2015, 95, 150-156.	10.3	24
114	Microfluidic spinning of editable polychromatic fibers. Journal of Colloid and Interface Science, 2020, 558, 115-122.	9.4	24
115	A portable ascorbic acid in sweat analysis system based on highly crystalline conductive nickel-based metal-organic framework (Ni-MOF). Journal of Colloid and Interface Science, 2022, 616, 326-337.	9.4	24
116	Antisolvent-Derived Intermediate Phases for Low-Temperature Flexible Perovskite Solar Cells. ACS Applied Energy Materials, 2018, 1, 6477-6486.	5.1	23
117	Composite Solid Electrolytes: Facilitating Interfacial Stability Via Bilayer Heterostructure Solid Electrolyte Toward Highâ€energy, Safe and Adaptable Lithium Batteries (Adv. Energy Mater. 31/2020). Advanced Energy Materials, 2020, 10, 2070131.	19.5	23
118	Highly efficient flexible perovskite solar cells made via ultrasonic vibration assisted room temperature cold sintering. Chemical Engineering Journal, 2020, 394, 124887.	12.7	23
119	Ultra-stretchable, self-adhesive, transparent, and ionic conductive organohydrogel for flexible sensor. APL Materials, 2021, 9, .	5.1	23
120	Solvent vapor annealing of oriented PbI2 films for improved crystallization of perovskite films in the air. Solar Energy Materials and Solar Cells, 2017, 166, 167-175.	6.2	22
121	NiCo–NiCoO2/carbon hollow nanocages for non-enzyme glucose detection. Electrochimica Acta, 2021, 381, 138259.	5.2	22
122	Reagentâ€Free Synthesis and Plasmonic Antioxidation of Unique Nanostructured Metal–Metal Oxide Core–Shell Microfibers. Advanced Materials, 2016, 28, 4097-4104.	21.0	21
123	Controllable construction of micro/nanostructured NiO arrays in confined microchannels via microfluidic chemical fabrication for highly efficient and specific absorption of abundant proteins. Journal of Materials Chemistry B, 2015, 3, 4272-4281.	5.8	19
124	Biocompatible and colloidally stabilized mPEG-PE/calcium phosphate hybrid nanoparticles loaded with siRNAs targeting tumors. Oncotarget, 2016, 7, 2855-2866.	1.8	19
125	A strong and flexible electronic vessel for real-time monitoring of temperature, motions and flow. Nanoscale, 2017, 9, 17821-17828.	5.6	19
126	Integrated Ionicâ€Additive Assisted Wetâ€Spinning of Highly Conductive and Stretchable PEDOT:PSS Fiber for Fibrous Organic Electrochemical Transistors. Advanced Electronic Materials, 2021, 7, 2100231.	5.1	19

#	Article	IF	CITATIONS
127	Three-Dimensional Clustered Nanostructures for Microfluidic Surface-Enhanced Raman Detection. ACS Applied Materials & Interfaces, 2016, 8, 24974-24981.	8.0	18
128	A flexible metallic actuator using reduced graphene oxide as a multifunctional component. Nanoscale, 2017, 9, 12963-12968.	5.6	18
129	ZnS–CdS–TaON nanocomposites with enhanced stability and photocatalytic hydrogen evolution activity. Journal of Sol-Gel Science and Technology, 2019, 91, 82-91.	2.4	18
130	High Volumetric Energy Density Asymmetric Fibrous Supercapacitors with Coaxial Structure Based on Graphene/MnO ₂ Hybrid Fibers. ChemElectroChem, 2020, 7, 4641-4648.	3.4	18
131	Stretchable electrothermochromic fibers based on hierarchical porous structures with electrically conductive dual-pathways. Science China Materials, 2020, 63, 2582-2589.	6.3	17
132	Bi ₂ Te ₃ Plates with Single Nanopore: The Formation of Surface Defects and Self-Repair Growth. Chemistry of Materials, 2018, 30, 1965-1970.	6.7	16
133	Defect-engineered bilayer MOFs separator for high stability lithium-sulfur batteries. Journal of Alloys and Compounds, 2021, 874, 159917.	5.5	16
134	Mechanical design of brush coating technology for the alignment of one-dimension nanomaterials. Journal of Colloid and Interface Science, 2021, 583, 188-195.	9.4	15
135	Core-shell structured SiO2@ZrO2@SiO2 filler for radiopacity and ultra-low shrinkage dental composite resins. Journal of the Mechanical Behavior of Biomedical Materials, 2021, 121, 104593.	3.1	15
136	Electrochemical Actuators with Multicolor Changes and Multidirectional Actuation. Small, 2022, 18, e2107778.	10.0	15
137	Rapid formation of superelastic 3D reduced graphene oxide networks with simultaneous removal of HI utilizing NIR irradiation. Journal of Materials Chemistry A, 2015, 3, 9882-9889.	10.3	14
138	Reagent-Free Electrophoretic Synthesis of Few-Atom-Thick Metal Oxide Nanosheets. Chemistry of Materials, 2017, 29, 1439-1446.	6.7	14
139	Highly Aligned Molybdenum Trioxide Nanobelts for Flexible Thin-Film Transistors and Supercapacitors: Macroscopic Assembly and Anisotropic Electrical Properties. ACS Applied Nano Materials, 2019, 2, 1466-1471.	5.0	14
140	Flexible photodetector based on cotton coated with reduced graphene oxide and sulfur and nitrogen co-doped graphene quantum dots. Journal of Materials Science, 2019, 54, 3242-3251.	3.7	14
141	Scalable fluid-spinning nanowire-based inorganic semiconductor yarns for electrochromic actuators. Materials Horizons, 2021, 8, 1711-1721.	12.2	14
142	Laser irradiated self-supporting and flexible 3-dimentional graphene-based film electrode with promising electrochemical properties. RSC Advances, 2015, 5, 47074-47079.	3.6	13
143	Solvatochromic structural color fabrics with favorable wearability properties. Journal of Materials Chemistry C, 2019, 7, 4855-4862.	5.5	13
144	Independent dual-responsive Janus chromic fibers. Science China Materials, 2021, 64, 1770-1779.	6.3	13

#	Article	IF	CITATIONS
145	Multifunctional Mechanical Sensing Electronic Device Based on Triboelectric Anisotropic Crumpled Nanofibrous Mats. ACS Applied Materials & Interfaces, 2021, 13, 55481-55488.	8.0	13
146	Highly integrated fiber-shaped thermoelectric generators with radially heterogeneous interlayers. Nano Energy, 2022, 95, 107055.	16.0	13
147	Flow Effects on the Controlled Growth of Nanostructured Networks at Microcapillary Walls for Applications in Continuous Flow Reactions. ACS Applied Materials & Interfaces, 2015, 7, 21580-21588.	8.0	12
148	Three-dimensional ordered titanium dioxide-zirconium dioxide film-based microfluidic device for efficient on-chip phosphopeptide enrichment. Journal of Colloid and Interface Science, 2016, 478, 227-235.	9.4	12
149	Visibly vapor-responsive structurally colored carbon fibers prepared by an electrophoretic deposition method. RSC Advances, 2016, 6, 16319-16322.	3.6	12
150	Light-driven artificial muscles based on electrospun microfiber yarns. Science China Technological Sciences, 2019, 62, 965-970.	4.0	12
151	Highly efficient walking perovskite solar cells based on thermomechanical polymer films. Journal of Materials Chemistry A, 2019, 7, 26154-26161.	10.3	12
152	Controlled preparation of β-Bi2O3/Mg–Al mixed metal oxides composites with enhanced visible light photocatalytic performance. Research on Chemical Intermediates, 2020, 46, 5009-5021.	2.7	12
153	Microstructural origin of selective water oxidation to hydrogen peroxide at low overpotentials: a study on Mn-alloyed TiO ₂ . Journal of Materials Chemistry A, 2021, 9, 18498-18505.	10.3	12
154	Ultra-stable ionic-liquid-based electrochromism enabled by metal-organic frameworks. Cell Reports Physical Science, 2022, 3, 100866.	5.6	12
155	High power factor n-type Ag ₂ Se/SWCNTs hybrid film for flexible thermoelectric generator. Journal Physics D: Applied Physics, 2021, 54, 434004.	2.8	11
156	Controlling the transformation of intermediate phase under near-room temperature for improving the performance of perovskite solar cells. Solar Energy, 2019, 186, 225-232.	6.1	10
157	Enhanced fluorescence and heat dissipation of calcium titanate red phosphor based on silver coating. Journal of Colloid and Interface Science, 2015, 459, 44-52.	9.4	9
158	Anion effect on properties of Zn-doped CH3NH3PbI3 based perovskite solar cells. Solar Energy Materials and Solar Cells, 2021, 233, 111400.	6.2	9
159	Environmentâ€sensitive carbon nanotube/polymer composite microhydrogels synthesized via a microfluidic reactor. Journal of Applied Polymer Science, 2013, 127, 2422-2426.	2.6	8
160	Capillary force driven printing of asymmetric Na-ion micro-supercapacitors. Journal of Materials Chemistry A, 2020, 8, 22083-22089.	10.3	8
161	Unipolar-stroke Electrochemical Artificial Muscles. Advanced Fiber Materials, 2021, 3, 147-148.	16.1	8
162	An electrically controllable all-solid-state Au@graphene oxide actuator. Chemical Communications, 2016, 52, 5816-5819.	4.1	7

10

#	Article	IF	CITATIONS
163	Carbothermal conversion of selfâ€supporting organic/inorganic interpenetrating networks to porous metal boride monoliths. Journal of the American Ceramic Society, 2019, 102, 5746-5762.	3.8	7
164	Facile synthesis of 3D hierarchical micro-/nanostructures in capillaries for efficient capture of circulating tumor cells. Journal of Colloid and Interface Science, 2020, 575, 108-118.	9.4	7
165	Synthesis of Mesoporous (Ga _{1â`'} <i>_x</i> Ca _{1â`'} <i>_x</i> O <i>< Using Layered Double Hydroxides as Precursors for Enhanced Visibleâ€Light Driven H₂ Production. Chinese Iournal of Chemistry, 2017, 35, 196-202.</i>	sub>x4.9	ıbş)
166	Additionalâ€Heatingâ€Enhanced Largeâ€Scale Metallic Molybdenum Disulfide Nanosheet Exfoliation for Freeâ€Standing Films and Flexible Highâ€Performance Supercapacitors. ChemNanoMat, 2020, 6, 267-273.	2.8	4
167	Dielectrophoretic Assembly of Carbon Nanotube Chains in Aqueous Solution. Advanced Fiber Materials, 2021, 3, 312-320.	16.1	4
168	Continuous preparation of dual-responsive sensing fibers for smart textiles. Journal of Colloid and Interface Science, 2021, 597, 215-222.	9.4	4
169	Graphene-based implantable neural electrodes for insect flight control. Journal of Materials Chemistry B, 2022, 10, 4632-4639.	5.8	4
170	Eu doped Si-oxynitride fluorescent nanofibrous inorganic membranes with high flexibility. RSC Advances, 2015, 5, 101287-101292.	3.6	3
171	Mesoporous Pt/TiO2-xNx nanoparticles with less than 10 nm and high specific surface area as visible light hydrogen evolution photocatalysts. Journal of Sol-Gel Science and Technology, 2018, 87, 230-239.	2.4	3
172	Oriented attachment growth of monocrystalline cuprous oxide nanowires in pure water. Nanoscale Advances, 2019, 1, 2174-2179.	4.6	3
173	Highly fluorinated polyimide gate dielectric for fully transparent aqueous precursor derived In–Zn oxide thin-film transistors. Journal of Materials Science, 2020, 55, 15919-15929.	3.7	3
174	Redox-Active Ni(II) Nodes Induced Electrochromism in a Two-Dimensional Conductive Metal–Organic Framework. ACS Applied Electronic Materials, 2022, 4, 2915-2922.	4.3	3
175	A self-healing, Na+ sensitive and neuron-compatible fiber. Chemical Engineering Journal, 2020, 386, 124018.	12.7	2